ISBN: 978-3-95450-216-5 doi:10.18429/JACoW-eeFACT2018-TUOBB01

OPTICS ABERRATION AT IP AND BEAM-BEAM EFFECTS

K. Ohmi*, K. Hirosawa, Y. Funakoshi, H. Koiso, A. Morita, Y. Ohnishi, D. Zhou,
KEK/Soken-dai, Tsukuba, Japan

Abstract

Collision in SuperKEKB phase II commissioning has started in April 2018. Luminosity was lower than the geometrical value even in very low bunch current at the early stage. Linear x-y coupling at IP caused by skew of QCS was conjectured as error source. x-y coupling correction using skew corrector of QCS resulted in luminosity recover of 2 times. After the QCS skew correction, luminosity is still limited at relatively low bunch current. Nonlinear x-y coupling at IP is conjectured as a source of the luminosity limitation in the next stage. We discuss effects of linear and nonlinear x-y coupling at IP on the beam-beam performance.

INTRODUCTION

SuperKEKB is asymmetric e+e− collider, which consists of low and high energy rings (LER & HER) with the energies $E = 4$ and 7 GeV, respectively. The target luminosity is $L = 8 \times 10^{35}$ cm^{-2}s^{-1} at beam current $I_{+,tot} = 3.6$ A and $I_{-,tot} = 2.6$ A with the number of bunches $N_b = 2,500$. Two beams collide with half crossing angle $\theta_c = 41.5$ mrad. Beta function at Interaction Point (IP) is squeezed to $\beta_x^* \sim 30$ mm and $\beta_y^* \sim 0.3$ mm. Piwinski angle is $\theta_c \sigma_z/\sigma_x$ is very large ~20; so-called, nano-beam/ superbunch/ large Piwinski angle collision is adopted. Phase-I commissioning in 2016 was focused to start the operation of the two storage ring (LER and HER) without collision. In Phase-II commissioning started from March 2018, beam-beam collision and luminosity tuning were main subjects. β^* was squeezed step-by-step during the commissioning. Table 1 summarizes the parameters. The beam-beam tune shift $\Delta\nu_{x,y}$ in Phase-II is calculated by the emittance without collision. Beam-beam parameter $\xi_y \sim \Delta\nu_y$ estimated by the achieved luminosity is lower than the value; lower value is $\xi_{L,-} = 2r_e\beta_y^* L/(N_-\gamma_- f_{rep}) \sim 0.02$ due to a vertical emittance increase mainly in e+ beam at beam-beam collision..

Optics aberrations at the interaction point have affected the beam-beam performance since KEKB operation. The operation had been continued while scanning the IP optics parameters for most of the time in day-by-day. Correction of the aberrations should be also very important for SuperKEKB. We discuss correction of linear aberration done in Phase-II and nonlinear aberrations toward future commissioning, Phase-III.

LINEAR COUPLING CORRECTION AT IP IN PHASE-II OPERATION

Specific luminosity, which is bunch luminosity normalized by bunch current product, is used as a measure for the beam-beam performance. When the beam particles distribute Gaussian in the transverse plane, the specific luminosity is represented only by the rms beam size,

$$L_{sp} = \frac{L}{I_+ I_-} = \frac{1}{2\pi\sigma_{xc}\sigma_{yc}e^2 f_0}, \quad (1)$$

where the beam size is square mean of e± beams, $\sigma_{yc} = \sqrt{\sigma_{y+}^2 + \sigma_{y-}^2}$. For collision with a large crossing angle $\theta_c\sigma_z/\sigma_x \gg 1$, the horizontal beam size is effectively projection of the bunch length into horizontal plane: i.e., $\sigma_{x,eff} = \theta_c\sigma_z$, where θ_c is the half crossing angle. σ_{xc} is square mean of the effective horizontal size of the two beams. The specific luminosity is characterized by the vertical beam size and bunch length. We expect that the specific luminosity is given by the vertical beam size determined by the vertical emittance ε_y and β_y^*, when beam-beam effect is negligible. By increasing beam current, the beam-beam effect dominates. Vertical beam size blow-up due to the beam-beam interaction results decrease of the specific luminosity.

Table 1: Parameters for SuperKEKB

parameter	design		Phase-II	
	LER	HER	LER	HER
$N_\pm(10^{10})$	9	6.5	4.8	4.0
$\varepsilon_{x/y}$ (nm/pm)	3.2/8.64	4.6/13	2.1/21	4.6/30
$\beta^*_{x/y}$ (mm)	32/0.27	25/0.3	200/3	100/3
ν_z	0.0247	0.028	0.022	0.026
$\Delta\nu_x$	0.0028	0.0012	0.0073	0.0025
$\Delta\nu_y$	0.088	0.081	0.075	0.077
ξ_L	0.088	0.081	0.03	0.02
$\sigma_z\theta_c/\sigma_x$	24.7	19.4	12.1	11.6

Figure 1 presents the specific luminosity as function of beam current product at early stage of squeezing beta to $\beta_y = 4$ mm (June 10, 2018). Vertical beam size is measured by X-ray monitor for both beams. As the beta function at the monitor is well-calibrated, the beam size corresponds to the vertical emittance. The beam sizes written in the figure are calculated by the measured vertical emittance $\sigma_y^* = \sqrt{\varepsilon_y\beta_y^*}$ in each (total) current, where the number of bunches are 788. The specific luminosity calculated by Eq. (1) using the beam size is plotted by red stars. The specific luminosity disagrees at low current. This result means the beam size at IP is deviate from $\sqrt{\beta_y^*\varepsilon_y}$ geometrically. The discrepancy of the specific luminosity is small at high bunch current. Electron beam is enlarged strongly at high current. Peak luminosity was $L_{peak} = 1.2\times10^{33}$ cm^{-2}s^{-1} for 285mA(e−)x340mA(e+) at $N_b = 788$.

There are several possibility for the disagreement of the specific luminosity. Beam collision offset is scanned in

* ohmi@post.kek.jp

ISBN: 978-3-95450-216-5 doi:10.18429/JACoW-eeFACT2018-TUOBB01

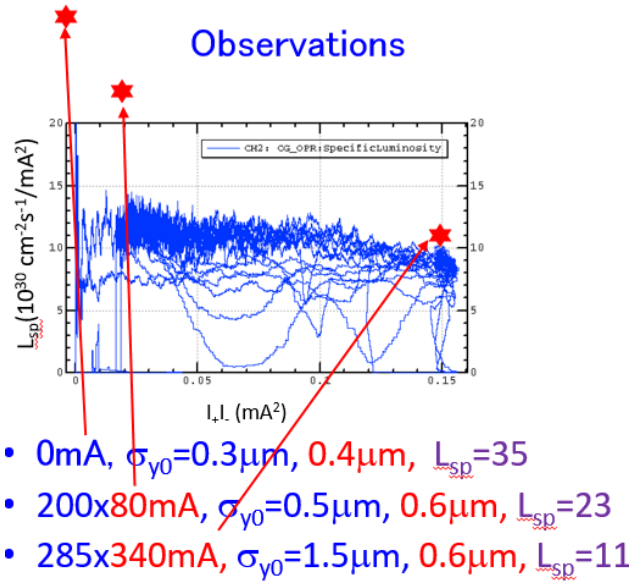

Figure 1: Specific luminosity as function of current product just after squeezing β^* =(200,4) mm.

x, y, z directions. β^* is checked by measurement at β at both side of final quadrupole magnets. Waist of β^* are scanned. Remained possibilities can come from local x-y coupling and vertical dispersion at IP.

x-y coupling is parameterized by R matrix for the 4×4 revolution matrix at IP.

$$M = RM_{2\times2}R^{-1} \tag{2}$$

where $M_{2\times2}$ is block diagonalized matrix, which is represented by β^*, α^* and ν in x and y plane. R matrix is represented by 4 parameters as

$$R = \begin{pmatrix} R_0 & 0 & R_4 & -R_2 \\ 0 & R_0 & -R_3 & R_1 \\ -R_1 & -R_2 & R_0 & 0 \\ -R_3 & -R_4 & 0 & R_0 \end{pmatrix} \tag{3}$$

where $R_0 = \sqrt{1 - R_1R_4 + R_2R_3}$.

R_1 characterizes rotation of beam in real $x-y$ space, while R_2 characterizes rotation in $x - p_y$ space. Figure 2 presents schematic view of collision at IP, where LER (positron) is ideal and HER (electron) has errors. Whether the rotation of the real space or the rotation of the momentum space, the beam size projected to y plane contributes to the luminosity.

The projected vertical beam size at IP in the presence of x-y coupling and vertical dispersion is expressed by

$$\sigma_y^2 = \varepsilon_y\beta_y + \varepsilon_x\beta_x\left(\frac{R_2^2}{\beta_x^2} + R_1^2\right) + (\eta_y\sigma_\delta)^2. \tag{4}$$

Correction of R_2

The specific luminosity at zero current was half of the prediction from the measured emittance as shown in Fig. 1.

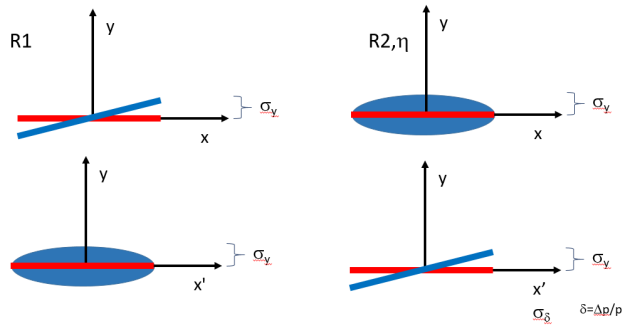

Figure 2: Phase space distribution of beam at IP in the presence of $R1, R2, \eta_y$. Red and blue depict distributions of positron and electron beam.

Electron beam was weak at high current: that is, errors seemed to exist in HER optics. It was conjectured that σ_y of electron beam was about 3 times larger than the nominal value $\sqrt{\varepsilon_y\beta_y^*}$ at zero current. Corresponding errors are estimated to be

$$R_1 = \pm30 \sim 60 \text{ mrad} \quad R_2 = \pm3 \sim 6 \text{ mm} \quad \eta_y = \pm1.5 \text{ mm}.$$

R parameters were changed by closed bump in arc sextupole magnets. Figure 3 presents luminosity, beam life time, vertical beam size for changing R_2. Luminosity increased, while life time and vertical beam size decreased for decreasing to $R_2 = -3.9$ mm. Optimum R_2 seemed to be further negative value. Increasing the bump height to change R_2 gives a side effect in vertical emittance increase due to induced vertical dispersion. We stopped to change R_2 to further negative direction at the first step.

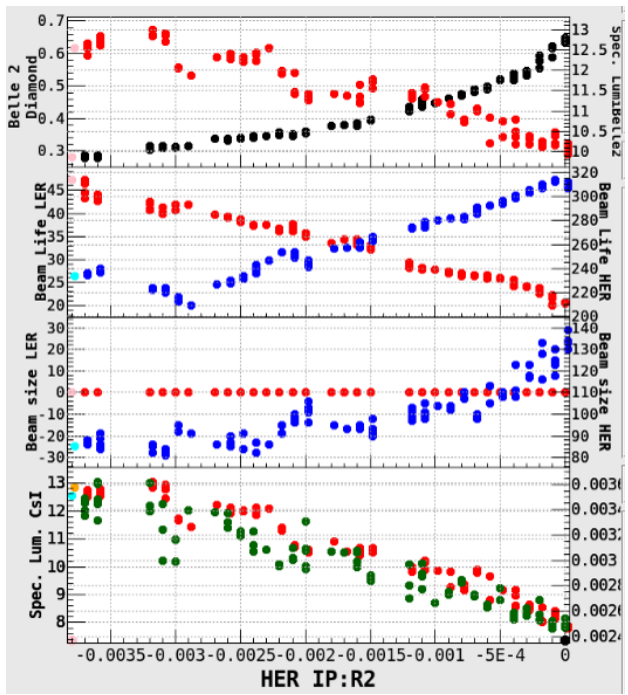

Figure 3: Luminosty, life time and beam size for r_2 scan.

ISBN: 978-3-95450-216-5 doi:10.18429/JACoW-eeFACT2018-TUOBB01

The linear transformation for R_2 is equivalent to

$$RM_{2\times2}R^{-1} = e^{-R_2 p_x p_y} M_{2\times2} e^{R_2 p_x p_y} \quad (5)$$

The source of R_2 seems to be skew of the final quadrupole magnets, QC1 or QC2. QC1 defocusing magnets are located at 0.6-1.9 m from IP. QC2 focusing magnets are located at 1.9-3.4 m from IP. Betatron phase difference between QC's and IP is about $\pi/2$ in both of $x-y$ plane as shown in Figure 4. Skew of QC magnets give a transformation with generating function of $H = ap_x p_y$. When both side of quadrupole magnets have rotation with the same angle but opposite direction, $a = \pm R_2$ ($\beta^*\beta(QC) \sim 1$), induced x-y coupling is confined in IR region and is invisible out side of IR. Transfer for H is $\bar{x} = x \pm R_2 p_y$, and $\bar{y} = y \pm R_2 p_x$, agree with the transfer matrix R in Eq. (3).

We do not change strength of IR magnets for squeezing β^*. R_2 induced by the rotation of QC is kept for squeezing β^*, because transfer from IP to QC's does not change. This means that the contribution to the beam size of R_2 in Eq. (4) is enhanced for squeezing β^*: that is, squeezing β^* results larger beam size at IP depending on R_2.

The correction of R_2 done by sextupole bump was replaced by exciting skew corrector in QC1. The skew corrector induces a small leak of R_3 component outside of IR, which was corrected by skew winding of sextupoles in arc. The side effect of the vertical emittance increase was eliminated.

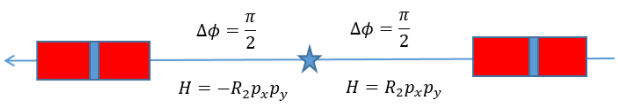

Figure 4: Transformatio for R_2.

We repeat to find optimum R_2 using sextupole bump and to correct the R_2 using skew corrector of QC1. R_2 was changed −7 mm in total. Figure 5 presents specific luminosity after the correction of R_2. Peak luminosity was $L_{peak} = 2.5\times10^{33}$ cm^{-2}s^{-1} for the same condition in Fig. 1, 285mA(e$^-$)×340mA(e$^+$) at $N_b = 788$. The luminosity gain is due to recovering the geometrical loss and relax a beam dynamical effect of R_2 at high current. Beam size blow-up in e$^+$ beam became stronger than that in e^- beam after the R_2 correction.

Measurement of x-y Coupling

x-y coupling is measured by turn-by-turn monitors. Beam is kicked by injection error, then the positions of the monitors is recorded. Horizontal betatron motion with ν_x is excited, and leaks in the vertical direction due to x-y coupling. There are 4 turn-by-turn monitors in IR section. Nearest monitors at IP (MQC1L-R) are placed inside of QC1. Using the left and right side of monitors, 4 dimensional phase space trajectory for the horizontal betatron motion at IP is solved. Figure 6 presents FFT signal given by the monitors. Top two plots show FFT amplitude of x, y position at Left and Right monitors. The signal with ν_x was seen in vertical of R

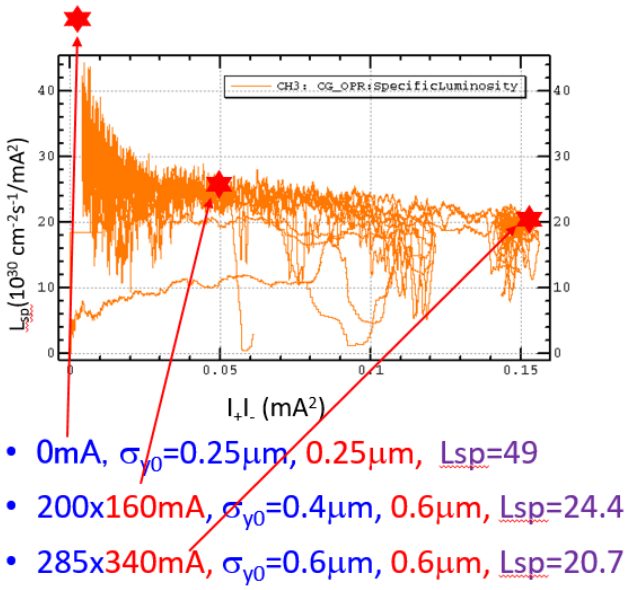

Figure 5: Specific luminosity as function of current product after r_2 correction.

and L monitors. Bottom two plots show FFT amplitude of x, y position and their slope $p = p_x = x', q = p_y = y'$ at IP. Roughly speaking, y_{IP} is evaluated by summation of y at left and right monitor, $y_L + y_R$, while q_{IP} is by difference of them, $y_L - y_R$. Clear signal for horizontal betatron motion was seen in q_{IP}, but was not in y_{IP}. R_1 and R_2 are evaluated by y_{IP} signal, while R_3 and R_4 are by q_{IP} signal. This result means that measurement of R_1 and R_2 is difficult compare with that of R_3 and R_4.

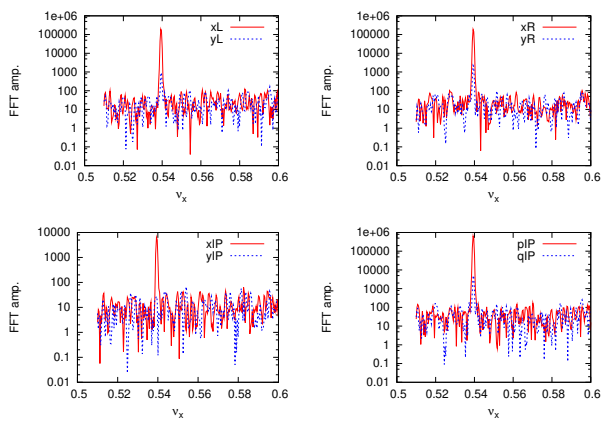

Figure 6: FFT amplitude for x and y signal of MQC1 monitors.

Figure 7 presents measured R_3 and R_4. Top two plot are given for HER and bottom plots are for LER. The measurement was performed for changing RF frequency (±200 Hz) also to evaluate their chromatic effect. The revolution frequency is $f_0 = 99.4$ kHz for $C = 3016$ m. The energy deviation is $\delta = \pm0.2$ %.

ISBN: 978-3-95450-216-5 doi:10.18429/JACoW-eeFACT2018-TUOBB01

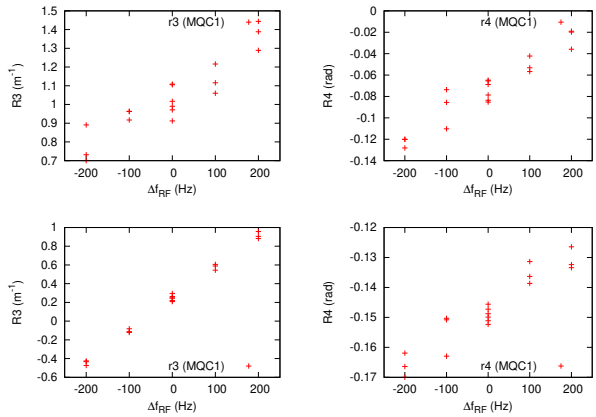

Figure 7: Measured R_3 and R_4 as function of RF frequency shift. Top two plot are given for HER and bottom plots are for LER.

The coupling parameters R_3 and R_4 and their chromatic components are obtained by fitting the measurement,

HER: $R_3 = 1.0 - 137\delta$ $R_4 = -0.073 - 23.3\delta$

LER: $R_3 = 0.24 - 338\delta$ $R_4 = -0.15 - 8.9\delta$.

TOWARD PHASE-III

Linear x-y coupling and vertical dispersion have been controlled well in the final stage of Phase II. The beam size at IP agreed with $\beta_y^*\varepsilon_y$ at collision with low bunch current ~0.01mA very well. However we still have luminosity degradation at high bunch current. Increase of the vertical emittance measured by X ray monitor well explains the luminosity degradation: that is, vertical emittance growth is caused by the beam-beam interaction. Emittance growth is not serious for beam-beam simulation without errors at IP, where the bunch current is still 50-60% of the design.

In experiments, e^+ beam has enlarged vertically at the end of Phase-II. We perform weak-strong simulation [1], in which e^+ beam is tracked in the fixed e^- beam force. In experiment, specific luminosity at the bunch current ($0.68\times0.57 = 0.39\text{mA}^2$) was around $L_{sp} = 15\times10^{30}\ \text{cm}^{-2}\text{s}^{-1}\text{mA}^{-2}$. The simulations were performed with applying IP errors to realized the degraded specific luminosity.

Figure 8 present the specific luminosity as function of bunch current product with/without linear x-y coupling. The specific luminosity without error is 29×10^{30} at the highest current 0.39 mA^2. Applied coupling parameters are written in the figure. R_1 and R_2 are possible errors in reality. We actually corrected R_2 with −7 mm. R_3 and R_4 which are measured by turn-by-turn monitor, are far smaller than the values $R_3 = 50\ \text{m}^{-1}$ and $R_4 = 2$. Errors of linear coupling parameters are not possible source of the luminosity behavior in Fig. 5.

Nonlinear coupling is possibility to explain the specific luminosity behavior. Assuming errors induced by QCS magnets, the nonlinearities are expressed by p_y at IP. Betatron phase difference deviate from $\pi/2$ in horizontal. Though p_x

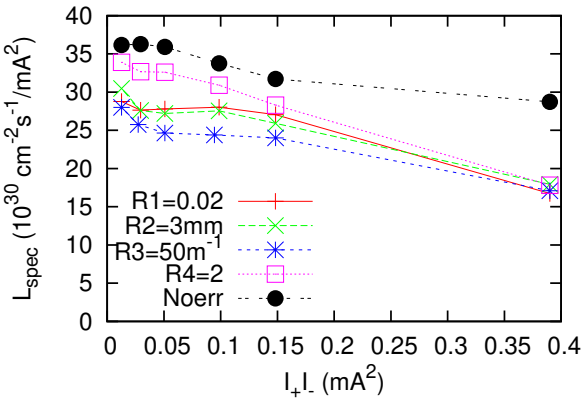

Figure 8: Specific luminosity as function of current product for linear aberrations obtained by weak-strong simulation.

terms are dominant, x terms should be taken into account. Figure 9 presents specific luminosity for considering 3-rd order terms; The transformation at IP are given by generating function,

$$H = c_1 p_x p_y^2 + c_2 p_x^2 p_y + c_3 p_y^3 + c_4 x^2 p_y. \qquad (6)$$

The specific luminosity for $p_x^2 p_y$ component agrees with the measurement of Fig. 5, The coefficient is $c_2 = 8$ m. The coefficient had evaluated in the design stage [2,3] was 0.07 m: that is, 100 times larger. The nonlinearity was induced at skew sextupole component of QC magnets and octupoles component of edge and body of their magnets in the presence of a vertical closed orbit.

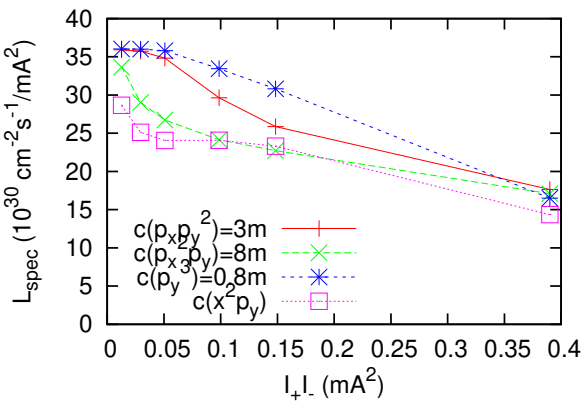

Figure 9: Specific luminosity as function of current product for nonlinear aberrations obtained by weak-strong simulation.

Another possibility is chromatic coupling. Figure 10 presents specific luminosity for chromatic coupling [4, 5]. The chromatic coupling for R_3 and R_4 are measured as shown in Fig. 7. The values $R_3' = 35{,}000$ and $R_4' = 1500$ are 100 times larger than the measurement. The behavior of the specific luminosity is different from the measurement in

ISBN: 978-3-95450-216-5 doi:10.18429/JACoW-eeFACT2018-TUOBB01

Fig. 5. For R_1' and R_2', the behaviors agree with the measurement. Measurement of R_1' and R_2' was difficult and has not performed yet.

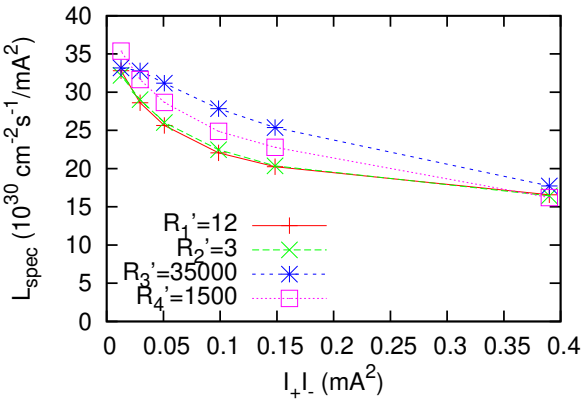

Figure 10: Specific luminosity as function of current product for chromatic coupling aberrations obtained by weak-strong simulation.

SUMMARY

SuperKEKB is squeezing β^* step-by-step in the commissioning of Phase II. Luminosity increase proportional to β_y^* is not trivial at all. Expected luminosity is only achieved, when the optics aberration at IP are perfectly corrected. QC magnet as error source and corrector is key component. Errors induced at QC magnets are enhanced for squeezing β^*. Correction of nonlinear aberration is next target in Phase-III commissioning.

The target specific luminosity in the design is $L_{sp} = 220\times 10^{30}$ cm^{-2}s^{-1}mA^{-2} at $I_+I_- = 1.5$ mA^2.

REFERENCES

[1] K. Ohmi et al., *Phys. Rev. ST-AB* 7, 104401 (2004).

[2] D. Zhou et al., in *Proc. IPAC'15*, paper WEYB3.

[3] K. Hirosawa et al., in *Proc. IPAC'18*, paper THPAK099.

[4] D. Zhou et al., *Phys. Rev. ST-AB* 13, 021001 (2010).

[5] Y. Ohnishi et al., *Phys. Rev. ST-AB* 12, 091002 (2009).